

# STARTER MOTOR SIZING FOR LARGE GAS TURBINE (SINGLE SHAFT) DRIVEN LNG STRINGS

by

**Bruce G. Heckel**

Manager, Systems Engineering

Elliott Turbomachinery Company Inc.

Jeannette, Pennsylvania

and

**Frank W. Davis**

Senior Rotating Equipment Engineer

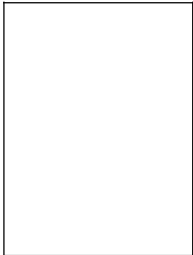
Ras Laffan Liquefied Natural Gas Company Ltd.

Doha, Qatar



*Bruce G. Heckel is the Manager of Systems Engineering for Elliott Turbomachinery Company, Inc., in Jeannette, Pennsylvania. He has worked for Elliott as a Compressor Product Engineer and later in Systems Engineering for a total of 32 years. Systems Engineering is responsible for the design of monitoring and control systems supplied with Elliott equipment.*

*Mr. Heckel has a B.S. degree (Mechanical Engineering) from the University of Pittsburgh (1964) and is a registered Professional Engineer in the State of Pennsylvania.*



*Frank W. Davis is a Turbomachinery Specialist with Mobil Oil Company (MEPTEC), assigned to Ras Laffan LNG Company Ltd., in Doha, Qatar. He has 30 years experience with machinery applications, design analysis, and troubleshooting with major oil companies.*

*Mr. Davis has a B.S. degree (Mechanical Engineering) from New Jersey Institute of Technology (1966) and is a registered Professional Engineer in the State of*

*New Jersey.*

## ABSTRACT

The purpose of this paper is to describe how computer simulation was used to size the main starter motors for single shaft gas turbine driven compressor strings used in a large LNG plant. The paper describes how the components of the system were modelled and discusses assumptions used in the calculations. The paper presents the actual computer output plots showing the predicted torque loading on the motor and the contributions of each of the components in the string to this predicted loading.

The simulation program was also used to predict the loading of the motor during a full load test at the compressor vendor's facility. A torque meter was used to measure the output of the motor during the string acceleration. The paper presents the results of the simulation prediction for the test runs and correlates the actual test measurements to the prediction.

## INTRODUCTION

The power requirements for mixed refrigerant (MR) and propane refrigeration compressors, as seen in the RasGas Qatar LNG Plant, have grown to the point where large, "single shaft gas turbines" have become the drivers of choice. The RasGas LNG Plant refrigeration duties are each over 75,000 BHP. Fortunately, the compressors can be directly connected to GE Frame 7 gas turbines, which have been designed for power generation service. Compared with a typical mechanical drive turbine, these turbines have a limited speed range and starting systems that are only capable of accelerating the gas turbine with an unloaded generator. Compressor capacity can be controlled by varying the turbine speed over its limited range and by control of gas recycle. Selection of the train starting scheme depends upon several factors that are discussed in this paper.

Economic use of a gas turbine for compressor drive services normally requires selection of the turbine design having a base load rating at plant ambient conditions that just exceeds the rated compressor power. If compressor power requirements exceed the site rating of available turbines, an additional helper driver can be utilized. This could be a steam turbine, variable frequency electric motor, or a second gas turbine. Such auxiliary drivers are available to supplement or replace the normal starting means for the principal gas turbine driver. For the application at RasGas LNG, the compression requirements could be met with a Frame 7 gas turbine, without the use of supplementary drivers.

The required train starting torque is determined by the system inertia, windage load of the gas turbine, the compressor gas loading during start, and the acceleration rate required for safe control of turbine temperatures. The Frame 7 is required to accelerate to 92 percent speed in approximately six minutes. At this speed, the turbine air compressor blowoff valves can be safely closed, and the turbine produces sufficient power to accelerate the full train load. The acceleration rate must be maintained within limits by the gas turbine control system, to avoid excessive thermal stresses. The conventional Frame 7 starting means does not provide adequate torque to accelerate this size of compressor train. The economic choice for a starting supplement was a variable frequency AC electric motor based upon hardware costs and machinery arrangement. The appropriate size of this motor was the subject of an evaluation of required train starting torque and available torque from the turbine and conventional starting system.

The implementation of the compressor starting procedures, the sizing and arrangement of recycle valves, the required acceleration rates, and the available supplemental torque identified by design

assumptions and economic analysis had to be confirmed by a dynamic simulation of the compressor train start. The power required by the process compressors is a function of the compressor speed, the flow through the compressor, and the density of the gas. The starting pressure and temperature directly affects the gas density and, therefore, the power requirements. Other factors that influence gas power include the volume of the suction, intermediate, and discharge systems, along with the pressure drops of each system.

For this study, Elliott has modelled the field piping systems along with gas turbine output torque characteristics based on an 800°F temperature drop across the turbine. This represents a moderate derating of the turbine design output to account for increased clearances with age and fouling of the air compressor and inlet filter. For the gas compressors, the minimum expected startup temperature was based on the minimum site water temperature for the gas coolers. Startup pressures for the compressor loops were selected to minimize subatmospheric pressure operation as the compressors reach rated speed. The compressor recycle valves, including startup bypasses where required, were sized large enough to permit the compressors to start in "stonewall." Stonewall is the compressor flow regime near choked flow where the pressure ratio and power are reduced.

In addition to supplying the power absorbed by the compressors, the variable speed starting motor must still have sufficient power left to accelerate the string at the required speed schedule. All the above factors were taken into account in Elliott's proprietary simulation program. The goal of the analysis is to produce a field startup speed/torque curve for the motor and thereby provide the basis for selecting the variable speed starting motor.

### SIMULATION COMPONENT MODELS

The simulation program comprises components that represent the various equipment of the string (Figure 1) and associated piping systems. The program interfaces all components of the system dynamically, thereby permitting evaluation of the entire system under various transient conditions including startup.

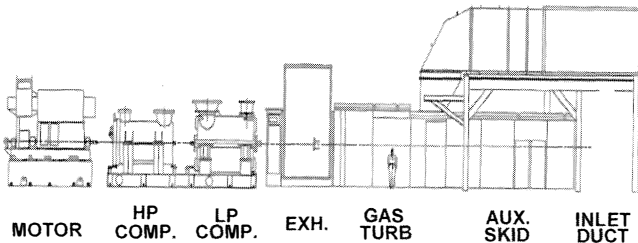


Figure 1. MR Compressor String.

The entire simulation program is designed around a building block concept. Each turbomachinery application is divided into discrete blocks for programming purposes. These blocks are assembled as subroutines in the configuration section of the program. All parameters are available to every part of the program by way of an "included common." This technique allows an unlimited number of configuration types from a variety of simulation component parts. These component parts are typically centrifugal compressors, axial compressors, steam turbines, gas expanders, gas turbines, various forms of control systems, various kinds of valves, piping, heat exchangers, and pressure vessels.

The computer program performs steady state and time transient calculations on mass flow, pressure, temperature, and rotative speed for the input model. Turbomachinery system dynamic characteristics are modelled by a series of first order differential equations. System transient response is evaluated in terms of control tuning parameters, piping configurations, and turbomachinery component characteristics.

The simulation utilizes lumped models based upon a control volume approach. Each compressor or turbine section has an inlet and discharge volume chamber with recycle, blowoff, venting, check valve, control valve, and block valve options. Pressure drops are considered to be concentrated at channels or points at the ends of a given chamber or volume. Pressure drops can be calculated from valve positions or input based upon system specification.

Each gas filled chamber or volume attached to a given turbomachinery component is solved with the continuity and energy equations, according to the characteristics of that interposing turbomachinery component. System rotative speeds are calculated from the power equation by considering the generated driver horsepower and the compressor system loads.

The energy equation is used to calculate the change in enthalpy internal to a given control volume or chamber, based upon enthalpy flux across the volume boundaries. The exit temperature of the given control volume, solved by an iteration process, is formulated by integrating an enthalpy balance equation in the time domain (Condrac, 1984).

$$T_d = \frac{1}{C_p M} \left[ \int_0^t \left[ \sum_{i=1}^n \dot{m}_i C_{pi} T_i \right]_{in} - \left[ \sum_{j=1}^m \dot{m}_j C_p T_d \right]_{out} dt + H_{ic} \right] \quad (1)$$

The continuity equation calculates the change of mass internal to the control volume based upon mass flow across the volume boundaries. The internal pressure of a chamber or volume is formulated by integrating this mass balance equation in the time domain and substituting the gas relation  $Pv = ZRT$  (Condrac, 1984).

$$P = \frac{ZRT}{VOL} \left[ \int_0^t \left[ \sum_{i=1}^n \dot{m}_i \right]_{in} - \left[ \sum_{j=1}^m \dot{m}_j \right]_{out} dt + M_{ic} \right] \quad (2)$$

The mass flow across chamber or volume boundaries is calculated from the pressure drop equation when a length of pipe is to be modelled (Condrac, 1984).

$$\dot{m} = K_d \sqrt{\frac{\Delta P}{v}} \quad (3)$$

When a control valve is utilized in the system to be modelled, the gas dynamic relation for flow through an orifice is used along with valve vendor flow data. This gas dynamic relationship calculates the mass flow through the valve as a function of pressure drop (Buresh and Schuder, 1964).

$$Q = \sqrt{\frac{520}{GTZ}} C_1 C_2 P_1 \sin \left[ \frac{59.64}{C_1 C_2} \sqrt{\frac{\Delta P_1}{P_1}} \right]_{rad} \quad (4)$$

The system rotative speed is calculated from a horsepower balance of the turbomachinery components on a given shaft. Bearing, windage, and disc friction losses are considered on the basis of each individual turbomachinery component. Therefore, for a rotating system, the speed response of a single shaft is defined by integrating in the time domain the power balance equation (Condrac, 1984).

$$N = \frac{C}{IN} \left[ \int_0^t \left[ \sum_{i=1}^n GHP_i \right]_{Driver} - \left[ \sum_{j=1}^m GHP_j \right]_{Load} dt \right] + N_{ic} \quad (5)$$

When a given model is constructed, all or some of the above equations are utilized to perform control and failsafe analyses. The simulation contains a number of algorithms for control system modelling. These algorithms can emulate industrial PID

controllers, lead/lag systems, integrators, lag derivative functions, second order systems, and first order systems. Valve actuator and sensor dynamics can be represented by any combination of these intermittent function algorithms.

Turbomachinery models, used internal to the simulation, are based upon state-of-the-art extended performance maps. Centrifugal compressors can be represented with polytropic head and polytropic efficiency versus volume flow maps generated for various speeds, or work (head/efficiency) versus volume flow maps generated for various speeds. The later has the advantage of being more linear at high flows and thereby easier for the simulation to converge on a solution. Since this application involves operation at high flows, the work curves were used.

In addition to the previously discussed relationships, refinements to the simulation theoretical calculations have been made based upon experience and empirical data. A combination of the knowledge of many disciplines, such as thermodynamics, aerodynamics, bearing design, electronics, and classical control theory, were brought together from the various engineering groups at the author's company in order to build the component models. Experience with valve and control system vendors has been utilized in order to develop sophisticated closed loop control models. The following is a summary of the major components.

*Gas Turbine*

The gas turbine is a single shaft design that is initially started with a small starter motor. The turbine is accelerated to about 30 percent speed for purging purposes and then decelerated to idle, at which point the combusters are ignited. The string is then reaccelerated using the starter motor to drive the string up to about 1000 rpm, at which time the main starter motor begins to contribute torque. The required speed schedule is shown in Figure 2. The gas turbine torque characteristics are shown in Figure 3. The torque characteristics are based on maximum ambient site conditions, with the compressor bleed valves open until above 91.5 percent speed. Note that the turbine becomes a power producer after approximately 60 percent speed.

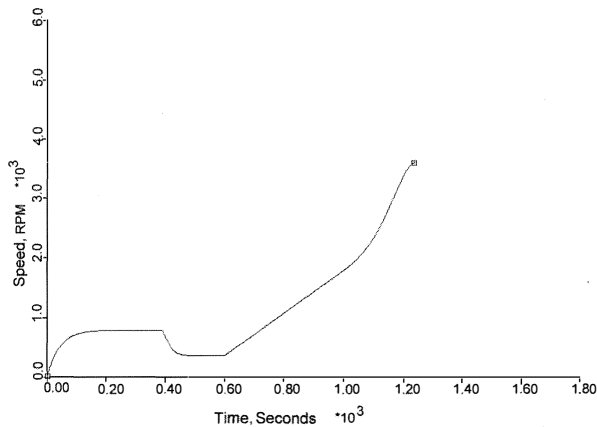


Figure 2. MR Compressor String Speed Schedule.

*Auxiliary Starter Motor*

The auxiliary starter motor drives the turbine through a torque converter. The gas turbine control system directs the torque converter to apply torque to the turbine shaft to accelerate the string, or remove torque to allow the string to decelerate. The auxiliary starter motor/torque converter output characteristic is shown in Figure 4.

*Compressors*

The startup philosophy used was to keep compressor pressure rise to a minimum, thereby reducing power requirements to

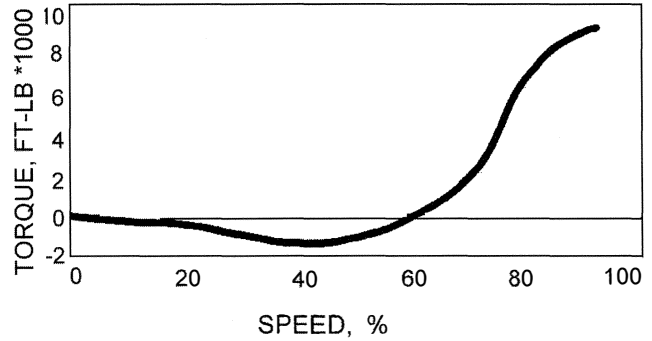


Figure 3. Gas Turbine Speed/Torque (Fired).

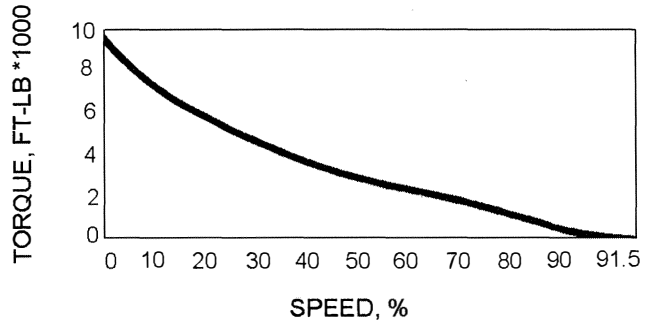


Figure 4. Auxiliary Starter Motor Speed/Torque.

downstream compressor sections, and to assist in preventing subatmospheric operation. Suction throttle valves were not used in order to avoid subatmospheric operation. The antisurge, or recycle, valves were sized large enough to cause compressor operation in stonewall (flows higher than design flow). The compressor characteristics were extended to high flows and zero head and are shown in Figure 5. The compressor model uses traditional methods to calculate compressor operating conditions and uses ideal gas properties. Ideal gas properties were used to keep simulation calculation times reasonable and were found to cause very little error, since discharge conditions did not change significantly during startup.

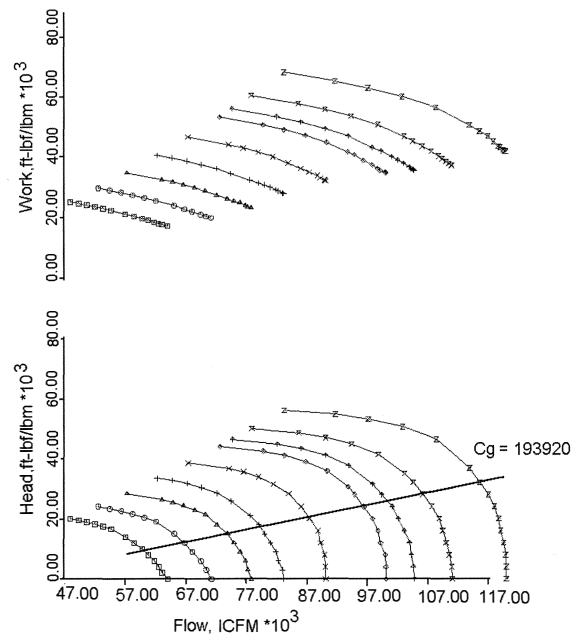


Figure 5. LP MR Compressor and Recycle Valve.

*Main Starter Motor*

The main starter motor is a variable speed synchronous motor that is used to supplement the available torque from the auxiliary starter motor and the turbine. It receives a signal from the gas turbine controller to make up the necessary torque in order to satisfy the speed schedule (Figure 2). The torque output for this motor is the net required to drive the compressor(s), less the amount contributed by the auxiliary starter motor and the gas turbine, plus the torque required to accelerate the string (considering rotational inertia of all string components) per the speed schedule. The simulation program predicts the motor loading as a function of speed for a given compressor loop starting pressure and recycle valve opening. This motor loading is the primary design criteria in the selection of the motor (Ekstrom and Garrison, 1993).

*Compressor Piping and Associated Components*

All elements of the piping system are modelled as volumes and associated pressure drops. The control valve model uses a valve sizing equation to predict valve pressure drops for a given  $C_v$ . The cooler model calculates the heat transfer as a function of cooling liquid flow and temperature, and predicts process gas temperature as a function of inlet flow and temperature.

**SIMULATION RESULTS**

*MR String*

A schematic of the MR string piping arrangement is shown in Figure 6. These components were modelled as described above. During startup, the isolation valves for each compressor are closed, the antisurge valves opened, and the pressure of the process gas in the loops are vented to slightly above atmospheric pressure (17 psia). The antisurge valves were sized sufficiently large to result in compressor operation in the stonewall region during runup with the valves fully open ( $C_g = 52,633$ , Figure 7).

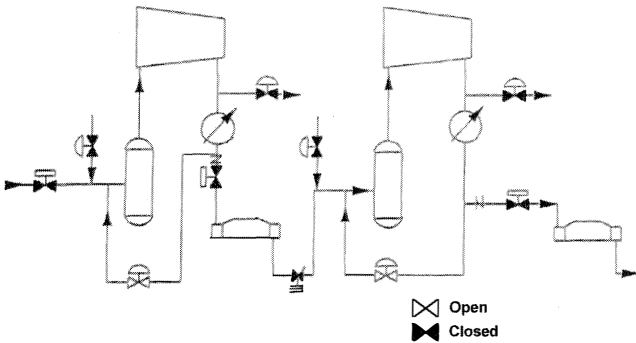


Figure 6. MR Compressor Circuit.

The simulation model used the same logic as that used in the gas turbine controller. The startup of the string consists of using the 1250 hp starter system, which is capable of turning the string up to approximately 1000 rpm, while the system purging is completed. The starter then decelerates the string to about 400 rpm, at which time the turbine combustors are ignited. Figure 8 shows the path traced by the various components during initial starting.

The 1250 hp auxiliary starter motor is indicated by 0-8, the 8 MW starter motor is shown as I-II, the gas turbine is depicted by a-d, and the LPMR compressor is identified as A-C with HPMR compressor as A-B. The speed schedule described earlier requires that contribution from the main starter motor (8 MW) is required after reaching approximately 1100 rpm.

The torque versus speed for all components covering the entire startup transient is shown in Figure 9. The gas turbine begins to make a positive contribution to string driving torque after

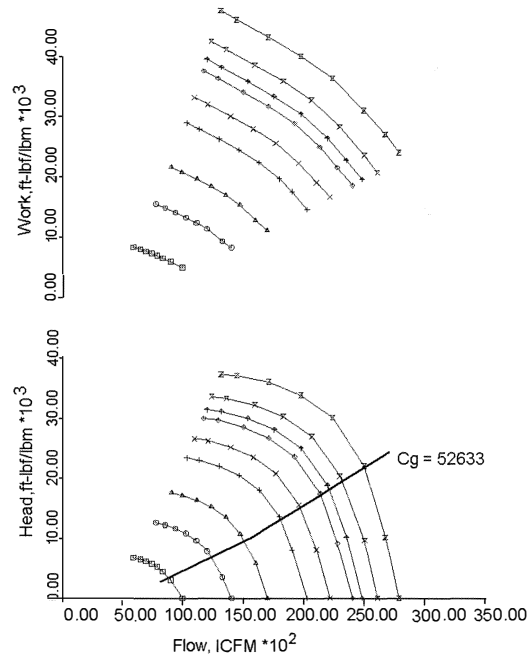


Figure 7. HP MR Compressor and Recycle Valve.

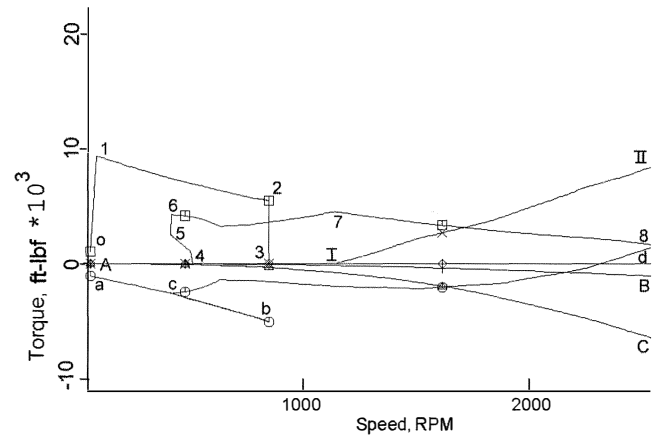


Figure 8. MR Enlarged Speed/Torque Curve.

approximately 2250 rpm. After reaching 91.5 percent speed (3294 rpm), the gas turbine bleed valves are closed and the 8 MW starter motor torque contribution is ramped down. The gas turbine picks up the load from the motor and continues to accelerate the string per the speed schedule. Once the turbine reaches minimum governor speed, the speed is held constant. The 8 MW motor makes up the difference in torque required to drive the compressors, less the contribution from the gas turbine and the 1250 hp auxiliary starter. The motor torque versus speed curve (shown in Figure 9) for the 8 MW starter motor is enlarged as Figure 10. This curve is the total requirement for the 8 MW starter motor, including accelerating torque necessary to meet the required speed schedule. (Note the maximum torque capability for the 8 MW motor is 15,500 ft-lb).

Figure 11 shows the suction and discharge pressures for the LPMR and HPMR compressors as a function of time. The results indicate that with the antisurge valves open and sized as indicated above, the LPMR suction pressure will fall just below 15 psia (at 91.5 percent speed), if initial starting pressure is 17 psia. Therefore, it may be necessary to slightly increase starting pressure or bleed in gas at speeds above 3400 rpm to avoid subatmospheric operation.

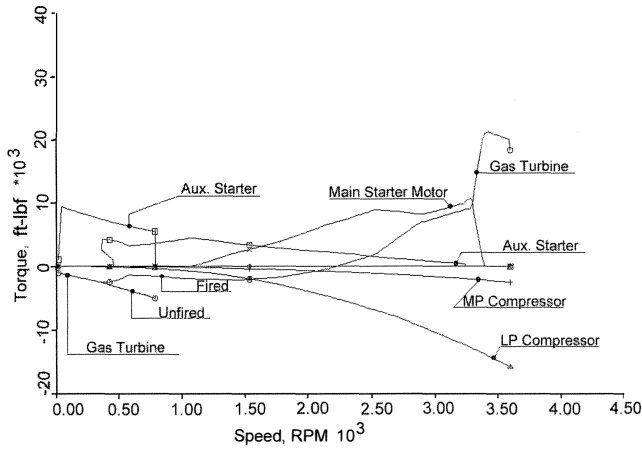


Figure 9. MR Compressor String—Speed/Torque.

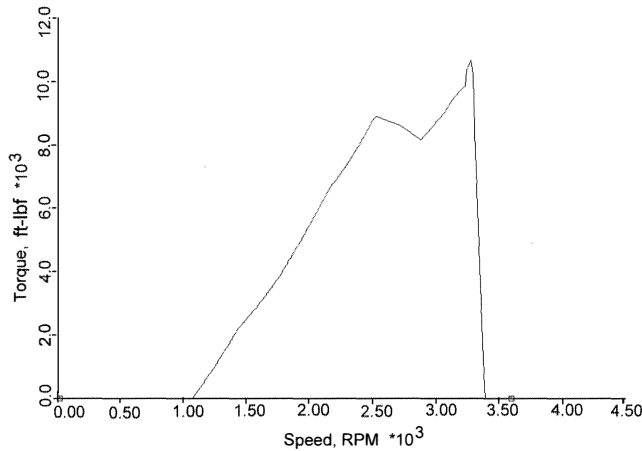


Figure 10. MR Compressor String—Motor Speed/Torque.

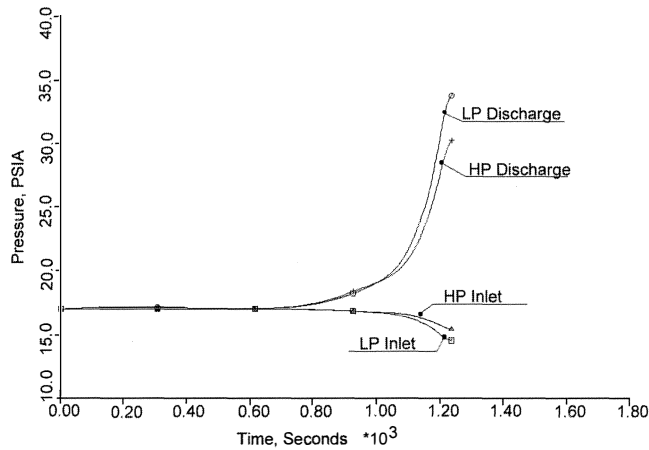


Figure 11. MR Compressor—Flange Pressures.

Propane String

The schematic of the propane string piping arrangement is shown in Figure 12. These components were modelled as described in the previous section SIMULATION COMPONENT MODELS, and are very similar to the MR compressor components. The main difference involves the compressor piping arrangement and valve sizing. The propane compressor is a three section compressor with a main inlet and two side streams. During startup, all valves shown are closed except the first section

antisurge valve and a large bypass around this valve. These valves are large enough to start the compressor in deep stonewall (all sections), which causes high volume flow, but keeps the second and third section inlets and final discharge pressure at a minimal pressure increase above the first section inlet (minimum head). Therefore, the mass flow to the second and third sections is significantly lower (no side load flows) than the design mass flows. Since the valves are very large, the pressure rise (head rise) is kept to a minimum, and the required starting pressure (to prevent extended subatmospheric operation) may also be minimized. The net result is to minimize the compressor torque without inlet throttling.

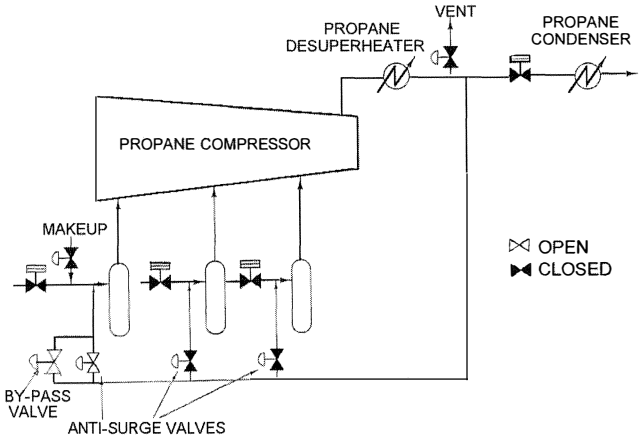


Figure 12. Propane Compressor Circuit.

A second difference involves the acceleration schedule of the gas turbine. The operation of the gas turbine is identical to that described previously for the MR string, except that it was necessary to slightly reduce the acceleration schedule for the gas turbine in the speed range just below the empowerment speed. The acceleration is a significant factor in total torque requirement for the starter motor. A comparison of the speed schedules for the two strings is shown in Figure 13. With the concurrence of the gas turbine vendor, the revised acceleration schedule resulted in reduced acceleration torque loading.

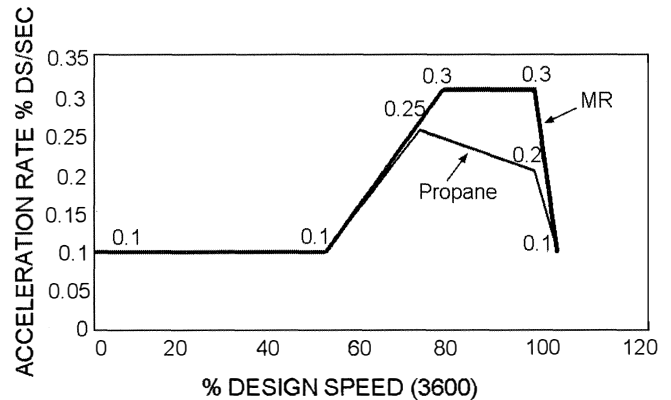


Figure 13. Gas Turbine Acceleration Rates.

Similar to the MR string, the propane string is isolated from the process and the gas is vented to a suitable starting pressure (15 psia) that will keep the starter motor sizing reasonable, while minimizing subatmospheric operation. With the antisurge valve and bypass valves open, the string is started and traces a path as shown on the performance curves (Figures 14, 15, and 16). The predicted flange pressures as a function of time are shown in Figure 17. The suction pressure falls to approximately 11.6 psia at the empowerment speed.

This pressure was judged acceptable as a short term situation. After reaching minimum governor speed, the loop pressure will be increased above atmospheric pressure. Figure 18 shows all torque contributing components plotted as a function of speed. The third compressor section torque could have been reduced further by using a larger bypass valve, thus reducing the section head and work. However, this would have required a much larger valve and would have only reduced the motor loading by approximately 15 percent. The motor speed torque curve (shown in Figure 18) is enlarged in Figure 19. A combination of the above factors contributed to lower torque requirements for the starter motor, which permitted the use of a duplicate (8 MW) starter motor as used on the MR string.

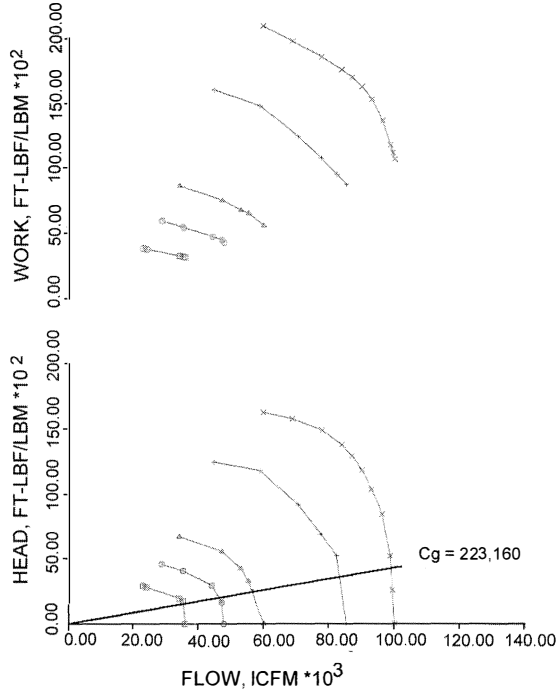


Figure 14. Propane Compressor Section 1 and Recycle Valve.

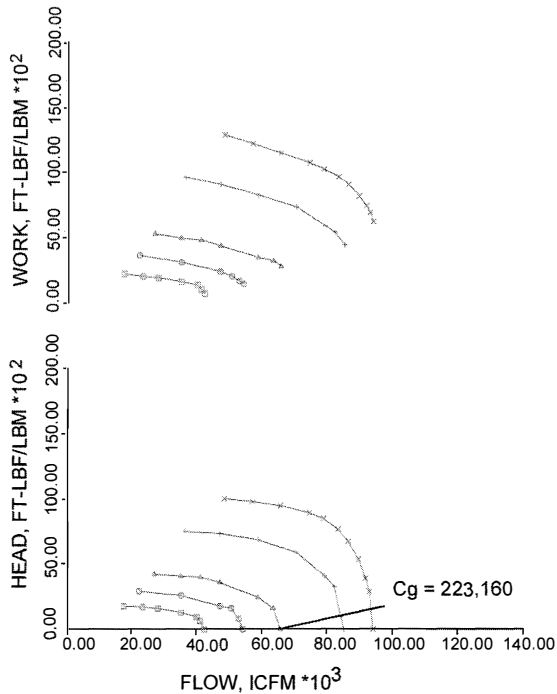


Figure 15. Propane Compressor Section 2 and Recycle Valve.

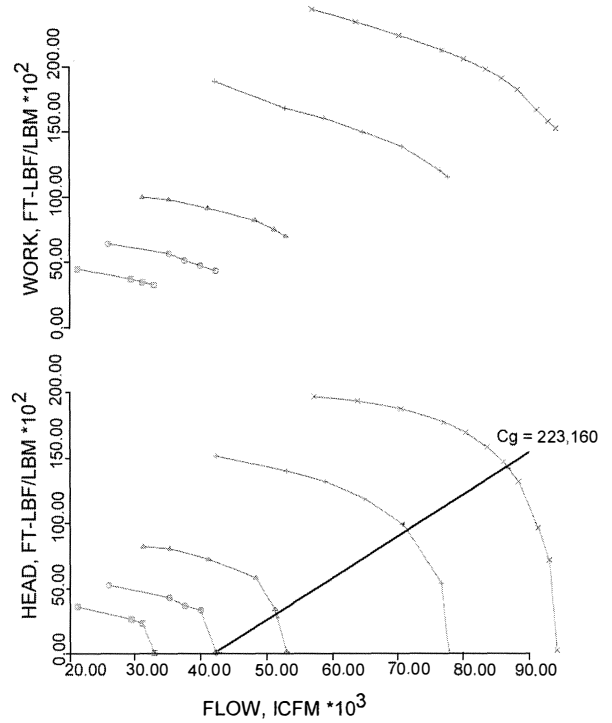


Figure 16. Propane Compressor Section 3 and Recycle Valve.

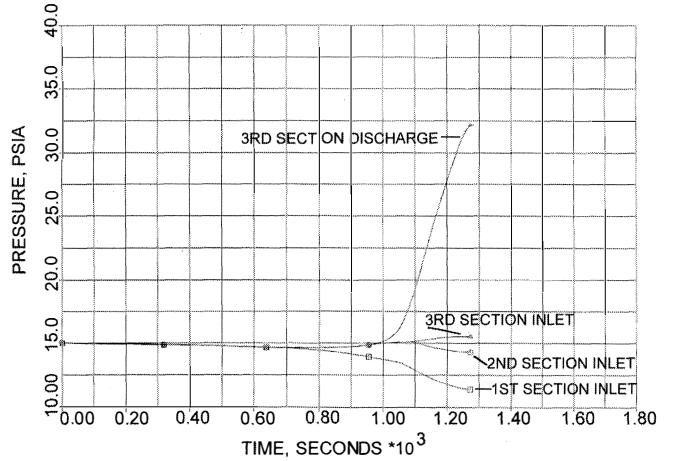


Figure 17. Propane Compressor Flange Pressures.

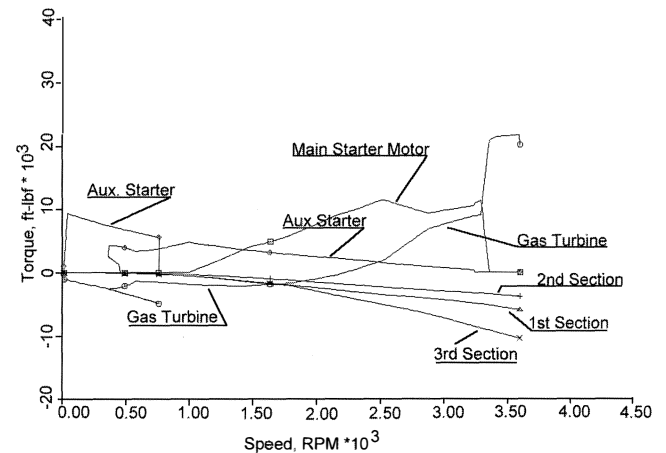


Figure 18. Propane Compressor String—Speed/Torque.

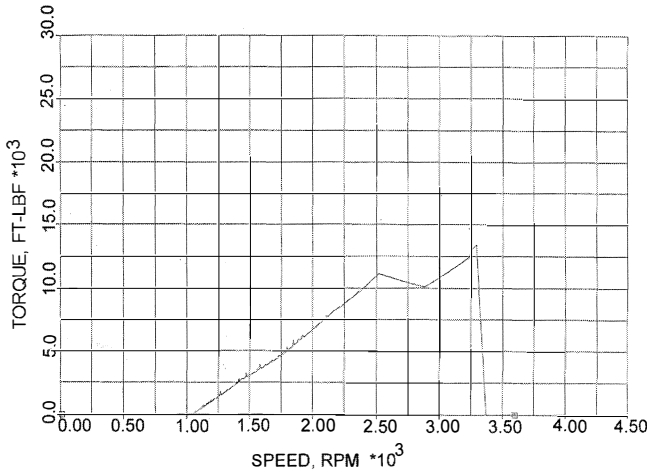


Figure 19. Propane Compressor String—Motor Speed/Torque.

TESTING

A full load mechanical test was specified for the compressors to demonstrate the overall mechanical design, prove the gas turbine and starting motor integrated control system, and to verify the engineering procedures utilized to size the starter motor. The design operating pressures and temperatures could not be duplicated with the inert (CO<sub>2</sub>) gas used for the full load test. Also, the gas turbine torque output for the test was expected to be much higher than the predicted field output, as the test ambient temperature is considerably lower than site temperatures. In addition, the turbine, as tested, was in a new, clean condition as compared with the condition used for design and simulation, which assumed a deteriorated turbine output (due to worn clearances and a dirty compressor and air filter).

It was decided to set the compressor test starting pressures and flows to emulate the peak compressor (field condition) torque during the starting cycle. Matching predicted compressor load during the test would verify the technique used for simulation and compressor load predictions during compressor start, when the stage flows and pressure ratios are near stonewall.

The predicted compressor loading during test was established through the use of the simulation program, as described above. The string was assembled on the test floor in the field configuration, with the exception that the coupling between the main starter motor and the compressor was modified to include a torquemeter. The torquemeter was needed to accurately measure the motor torque during the acceleration to the self sustaining speed.

MR Compressor String

The test arrangement for the MR compressor string is shown in Figure 20. The compressor bodies were totally isolated during the testing. The main and bypass valves in the compressor discharges were sized to emulate the field antisurge valves. The valving was large enough to load the compressors in the stonewall region. Table 1 shows a summary of the field startup simulation (Run 2e) that was the basis for the main starter motor selection. The predicted compressor torque at 3280 rpm is 16,189 ft-lb. Multiple simulation runs were made in an attempt to emulate the field conditions, matching head and torque as close as possible for the test gas conditions. It was not possible to also match the compressor volume flows, due to the differing characteristics of the test gas as compared with the field gas. A summary of the simulation run that most closely approximates the field startup conditions is shown as Run 34. The desired loading was achieved by establishing a setting for the discharge throttle valve and loop starting pressures and temperatures. The gas turbine acceleration rate was set in the turbine controls to simulate the design rate.

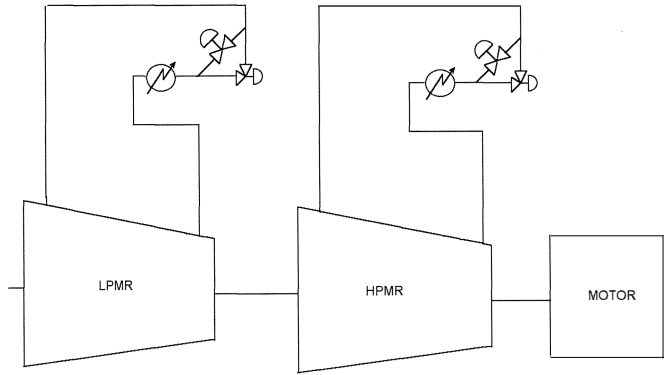


Figure 20. MR Test System Arrangement.

Table 1. MR Simulation Versus Test Results.

PARAMETER	SIMULATION		TEST RESULTS	
	FIELD LP/HP	TEST LP/HP	COLD START	HOT START
Run Number	2e	34	Point 3	Point 9
Speed (rpm)	3280	3280	3280	3280
Inlet Pressure (psia)	15.12/16.34	8.24/8.31	8.1/8.9	8.4/8.7
Inlet Temperature (°F)	7575	100/100	64/65	63/64
Inlet Flow (scfm)	94432/19564	110796/22647	110925/25400	110173/24980
Discharge Pressure (psia)	39.34/33.95	34.78/22.74	32.1/24.4	32.8/23.9
Discharge Temperature (°F)	192/154	360/275	318/220	324/232
Head (ft./#)	33445/23893	34408/22706	31312/21250	30994/21470
Efficiency (%)	76/81	78/79	73.8/84.7	71.2/78.9
Gas/MW	Mix/25.88	CO <sub>2</sub> /44.01	CO <sub>2</sub> , Air/43.87	CO <sub>2</sub> , Air/44.009
Horsepower (each section)	8761/1350	8888/1248	9045/1347	9601/1407
Horsepower (total-incl. losses)	10111	10136	10560	11176
Motor Full Load Torque (ft.-lb.)	15500	15500	15500	15500
(1) Compressor Torque (total- ft.-lb.)	-16189	-16229	-16909	-17896
(2) Gas Turbine Torque (ft.-lb.)	9008	9010	18273	20810
(3) Accelerating Torque (ft.-lb.)	-4937	-4935	-5064	-5064
Motor Torque (ft.-lb.)	12118	12154	3700	2150
Starting Pressure (psia)	18.1/18.1	16.5/15.5	16.5/15.5	16.5/15.5
Starting Temperature (°F)	7575	100/100	80/76	113/94

Pressures and temperatures at the compressor inlet and discharge along with flow and the motor torque were recorded on a high speed data acquisition system. The results of the startup test are shown in Table 1 (Point 3 and Point 9). Plots of motor torque, string acceleration, compressor pressures, and compressor flows are shown in Figures 21, 22, 23 and 24. In order to verify that the compressor power was representative of the predicted field conditions, an ASME PTC 10 based performance point was taken just after reaching minimum operating speed (3420 rpm). The calculated power at minimum operating speed was then fan law corrected to the empowerment speed (3280 rpm). Comparing the simulation prediction (run 34) with the test results (point 3) shows that the measured compressor torque during test of 16,909 ft-lb was just slightly higher than prediction (16,229 ft-lb). Similarly, the actual accelerating torque (5064 ft-lb) was slightly higher than the predicted (4935 ft-lb). However, as expected, the measured motor torque (3700 ft-lb) was considerably less than predicted (12,154 ft-lb), due to the expected higher turbine output.

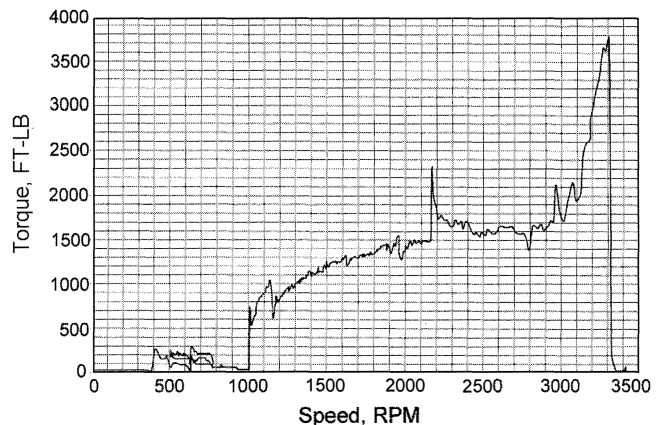


Figure 21. MR Motor Speed/Torque Test Results.

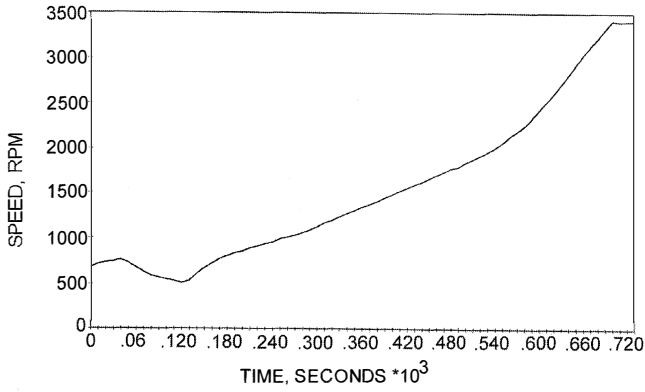


Figure 22. MR String—Speed Versus Time.

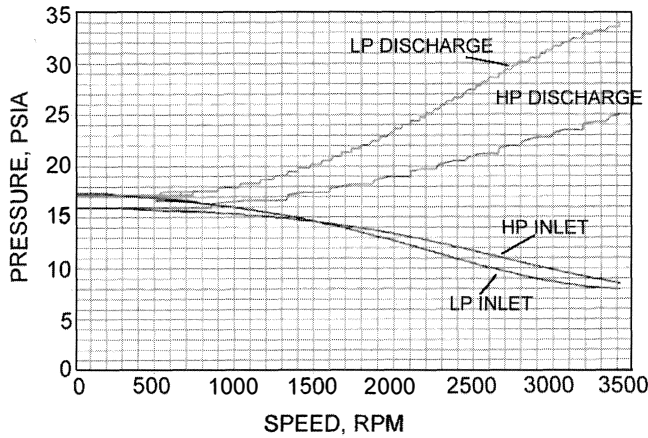


Figure 23. MR Compressors Test—Pressure Versus Speed.

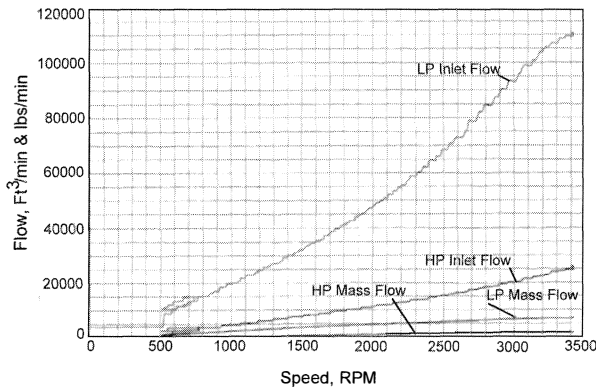


Figure 24. MR Compressors Test—Flow Versus Speed.

**Propane Compressor String**

The test arrangement for the propane compressor string is shown in Figure 25. During startup, the side load valves were fully closed and the main inlet and bypass valves were positioned to emulate field loading on the compressor. These valves were sufficiently large to load the compressor in deep stonewall. Table 2 shows a summary of the field startup simulation (Run 12) that was the basis for the main starter motor selection. The predicted compressor torque at 3293 rpm is 19,135 ft-lb. Multiple simulation runs were made in an attempt to emulate the field conditions, matching head and torque as close as possible for the test gas conditions. It was not possible to also match the compressor volume flows, due to the differing characteristics of the test gas as compared with the field

gas. A summary of the simulation run that most closely approximates the field startup conditions is shown as Run 19. The desired loading was achieved by establishing a setting for the discharge throttle valve and loop starting pressures and temperatures. The gas turbine acceleration rate was set in the turbine controls to simulate the design rate.

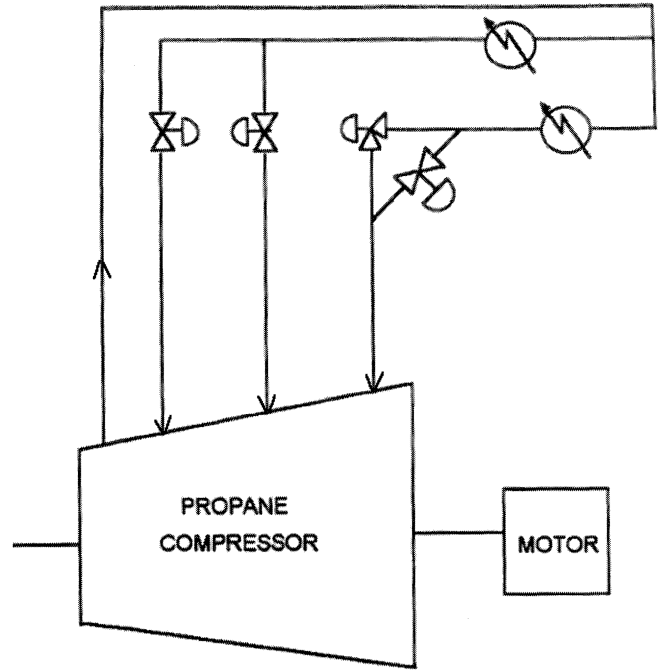


Figure 25. Propane Test System Arrangement.

Table 2. Propane Simulation Versus Test Results.

PARAMETER	PROPANE - TRANSIENT START-UP			
	SIMULATION PREDICTIONS		TEST RESULTS	
	FIELD	TEST	COLD START	HOT START
Run Number	12	19	7	13
Speed (rpm)	3293	3290	3290	3290
Inlet Pressure (psia)	11.69	12.12	12.2	11.8
Inlet Temperature (°F)	75	80	75	73
Inlet Flow (icfm)	101851	100746	93461	96420
Discharge Pressure (psia)	29.05	27.17	28.8	28.1
Discharge Temperature (°F)	205	330	331	329
Head (ft #/W)	18925	18759	19999	20020
Efficiency (%)	43	45	46	47
Horsepower (total-incl. losses)	12005	12050	11764	11918
Motor Full Load Torque (ft.-lb.)	15500	15500	15500	15500
(1) Compressor Torque (total- ft.-lb.)	-19135	-19231	-18780	-19026
(2) Gas Turbine Torque (ft.-lb.)	9033	9028	14237	17432
(3) Accelerating Torque (ft.-lb.)	-3281	-3286	-3789	-3995
Motor Torque (ft.-lb.)	13383	13489	8332	5589
Starting Pressure (psia)	15.0	17.55	17.5	17.5
Starting Temperature (°F)	75	80	75	95

Pressures and temperatures at the compressor inlet and discharge along with flow and the motor torque were recorded on a high speed data acquisition system. The results of the startup test are shown in Table 2 (Run 7 and Run 13). Plots of motor torque, string acceleration, compressor pressures, and compressor flows are shown in Figures 26, 27, 28, and 29. In order to verify that the compressor power was representative of the predicted field conditions, an ASME PTC 10 based performance point was taken just after reaching minimum operating speed (3420 rpm). The calculated power at minimum operating speed was then fan law corrected to the empowerment speed (3290 rpm). Comparing the simulation prediction (Run 19) with the test results (Run 7) shows that the measured compressor torque during test of 18,780 ft-lb was just slightly lower than prediction (19,231 ft-lb). Similarly the actual accelerating torque (3789 ft-lb) was slightly higher than the predicted (3286 ft-lb). However, as expected, the measured motor torque (8332 ft-lb) was considerably less than predicted (13,489 ft-lb), due to the expected higher turbine output.



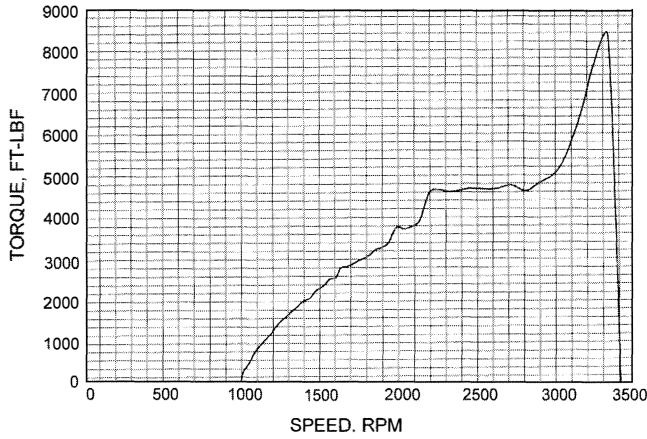


Figure 26. Propane Motor Speed/Torque Test Results.

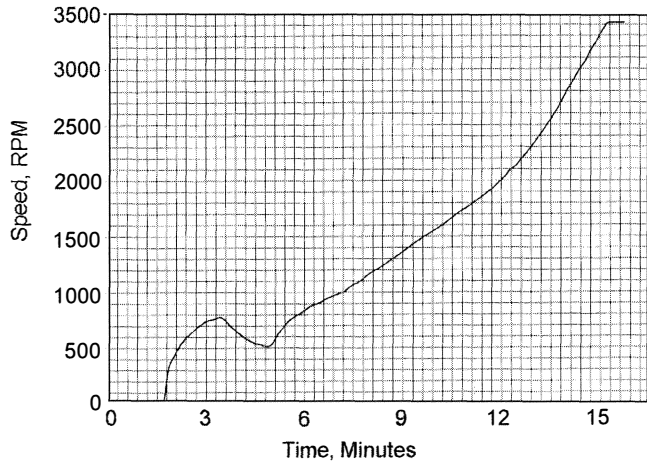


Figure 27. Propane String—Speed Versus Time.

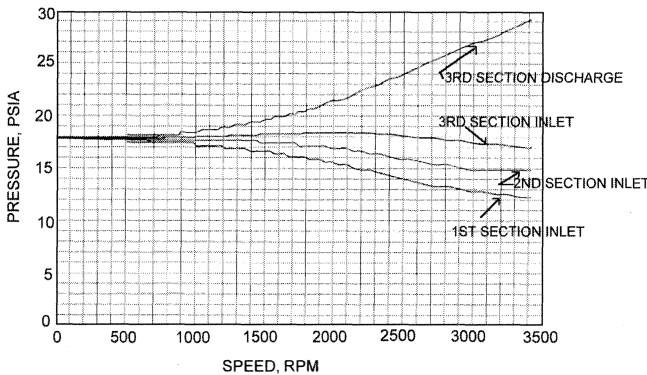


Figure 28. Propane Compressors Test—Pressure Versus Speed.

**CONCLUSION**

This paper describes the characteristics of the major components of the mixed refrigerant and propane strings, how the simulation program was used to model these components, how the results of the simulation were used to select the main starter motor, and a comparison of the full load test results with the simulation prediction.

The torque balance relationship for the MR string is shown in Figure 9 and the propane string in Figure 18. The auxiliary starter motor is used to accelerate the string to approximately 800 rpm for purge purposes, then decelerate the string to approximately

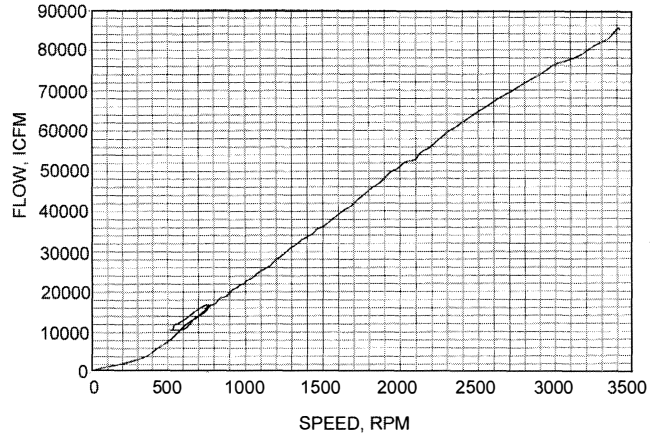


Figure 29. Propane Compressors Test—Inlet Flow Versus Speed.

400 rpm, at which time ignition occurs and the string is accelerated per the programmed schedule in the gas turbine (Figures 1 and 13). The gas turbine absorbs power up until approximately 2250 rpm. Above this speed, it begins to produce power in a nearly linear relationship with speed, until reaching 91.5 percent design speed. At this speed, the turbine bleed valves are closed, and the gas turbine is able to absorb full design load. As can be seen, the gas turbine and the auxiliary starter motor do not have sufficient torque capability to drive the total torque requirement of the compressors (LP MR and HP MR). In addition, a torque of approximately 4935 ft-lb is required to accelerate the string at the required rate. The shortfall is made up by the main starter motor. The torque requirement for the main starter motor peaks at the 91.5 percent speed and is ramped to zero as the gas turbine picks up the load.

The use of the simulation program to predict starter motor loading during runup of the gas turbine driven strings proved to be an invaluable tool. It was also used to predict string component loading during full load test startup, so that representative compressor loading could be established emulating field conditions. Simulation results showed that the propane compressor could be started without the use of an inlet throttle valve, with both side loads closed, and do so at considerably reduced power without surging. This was verified by the testing.

The results of the load test demonstrated that the design assumptions of compressor starting torque (deep stonewall loading), which were used in the simulation, were accurate. Good correlation between the simulation results and test results was shown except for the higher than predicted gas turbine output. This, however, was explainable due to lower test ambient temperatures and an as-new condition. Test results also proved that the compressor pressure and flow conditions defined by the startup simulation study can safely be utilized for sizing of the compressor recycle and bypass valves.

**NOMENCLATURE**

- A Area
- C Speed equation constant
- $C_p$  Specific heat at constant pressure
- $C_v$  Flow coefficient
- $C_1$   $C_g/C_v$
- $C_2$  Correction factor for variation in specific heat ratio, k
- G Gas specific gravity
- GHP Gas horsepower
- $H_{ic}$  Bulk enthalpy initial condition
- I Shaft rotational inertia
- K Ratio of specific heats
- $K_d$  Pressure drop constant
- $\dot{m}$  Mass flowrate
- M Mass of gas in a control volume

$M_{ic}$	Mass of gas in a control volume at initial condition
$N$	Rotative shaft speed
$N_{ic}$	Rotative shaft speed at initial condition
$P$	Internal pressure of control volume
$P_1$	Valve inlet pressure, psia
$P_2$	Valve outlet pressure, psia
$\Delta P$	Pressure drop
$\Delta P_1$	Differential pressure across valve, psi
%P	Proportional band
PR	Pressure ratio
Q	Gas flowrate, scfh
R	Gas constant
t	Time
T	Temperature into or out of control volume
$T_1$	Absolute temperature of gas at valve inlet, °R
$T_d$	Exit temperature
$T_r$	Reset time
v	Specific volume
VOL	Internal volume
Z	Compressibility factor

## REFERENCES

- Buresh, J. F. and Schuder, C. B., October 1964, "Development of a Universal Gas Sizing Equation for Control Valves," Reprinted from ISA Transactions, 3, (4), Fisher Controls Company, Marshalltown, Iowa.
- Condrac, E. J., March 26-28, 1984, "Digital Computer Modeling of Turbomachinery," Fluid Machinery Congress in the Hague, Elliott Company, Jeannette, Pennsylvania.
- Ekstrom, T. E. and Garrison, P. E., 1993, "Gas Turbines for Mechanical Drive Applications," GER-3701B, GE Industrial & Power Systems, Schenectady, New York.

## ACKNOWLEDGEMENTS

The following individuals provided a significant contribution to the writing of this paper and the successful completion of the design, manufacture, and testing of this equipment: Charles Colledge, Mike Gribbin, Ross Hackel, Nick Kosanovich, Dennis Paluselli, and Rege Stegman, Elliott Company, Jeannette, Pennsylvania.